



HAL
open science

Statistics of percolating clusters in a model of photosynthetic bacteria

Jean-Christian Anglès d'Auriac, Ferenc Iglói

► **To cite this version:**

Jean-Christian Anglès d'Auriac, Ferenc Iglói. Statistics of percolating clusters in a model of photosynthetic bacteria. *Physical Review E*, 2021, 103 (5), pp.052103. 10.1103/physreve.103.052103. hal-04158257

HAL Id: hal-04158257



<https://hal.science/hal-04158257>

Submitted on 11 Jul 2023

HAL is a multi-disciplinary open access archive for the deposit and dissemination of scientific research documents, whether they are published or not. The documents may come from teaching and research institutions in France or abroad, or from public or private research centers.

L'archive ouverte pluridisciplinaire **HAL**, est destinée au dépôt et à la diffusion de documents scientifiques de niveau recherche, publiés ou non, émanant des établissements d'enseignement et de recherche français ou étrangers, des laboratoires publics ou privés.

Statistics of percolating clusters in a model of photosynthetic bacteria

Jean-Christian Anglès d'Auriac ^{1,*} and Ferenc Iglói ^{2,3,†}

¹*Institut Néel-MCBT CNRS, Boîte Postale 166, F-38042 Grenoble, France*

²*Wigner Research Centre for Physics, Institute for Solid State Physics and Optics, P.O. Box 49, H-1525 Budapest, Hungary*

³*Institute of Theoretical Physics, Szeged University, H-6720 Szeged, Hungary*



(Received 21 January 2021; accepted 15 April 2021; published 3 May 2021)

In photosynthetic organisms the energy of the illuminating light is absorbed by the antenna complexes and transmitted by the excitons to the reaction centers (RCs). The energy of light is either absorbed by the RCs, leading to their “closing” or is emitted through fluorescence. The dynamics of the light absorption is described by a simple model developed for exciton migration that involves the exciton hopping probability and the exciton lifetime. During continuous illumination the fraction of closed RCs x continuously increases, and at a critical threshold x_c , a percolation transition takes place. Performing extensive Monte Carlo simulations, we study the properties of the transition in this correlated percolation model. We measure the spanning probability in the vicinity of x_c , as well as the fractal properties of the critical percolating cluster, both in the bulk and at the surface.

DOI: [10.1103/PhysRevE.103.052103](https://doi.org/10.1103/PhysRevE.103.052103)

I. INTRODUCTION

In living organisms the conversion of (sun)light to chemical energy is performed during photosynthesis. In this process the absorption of photons takes place at the antenna complexes, followed by funneling the excitation energy (exciton) to a specially organized dimer P in the reaction centers (RCs) [1]. During the chemical reaction $P \rightarrow P^+$, when the RC becomes “closed,” the energy of the exciton is transferred to chemical energy [2–4]. Another exciton visiting the closed RC can be redirected to an open RC, and the exciton is able to visit several RCs during its lifetime. The search for utilization of excitons by photochemistry (charge separation) competes with loss by fluorescence emission. To describe theoretically this complicated cooperative process several simplified models have been introduced and studied [5–12].

In the first class of models homogeneous distribution of the closed (and open) RCs is assumed together with a small set of reaction rates [12,13]. Within this Joliot-Lavergne-Trissl model, the time dependence of the concentrations of P^+ is obtained by solving a set of ordinary differential equations. However, recent experiments [14] on the time dependence of the fluorescence yield show important deviations from the predictions of this standard theory. In a second class of models the exciton migration is treated in a more accurate way [9,15–19]. The disadvantage of these models is that numerical methods are needed to solve the equations, and the final results are often not directly related to measurable observables.

Recently, one of us proposed a simple model to describe the migration of the excitons and the closure of the RCs [14]. (Hereafter we refer to it as the exciton migration (EM) model.) This model goes beyond the homogeneous kinetic model and

accounts for the local topology of the RC lattice as well as the bunching effect of the closed RCs during light excitation (induction). The EM model was solved analytically using various reasonable approximations (standard mean-field, lattice mean-field, and cluster mean-field methods) and made comparing the theoretical predictions with the experiments possible.

Despite its possible experimental relevance, the EM model also has several theoretical challenges. One of those is the question of the structure of the closed RCs. During induction the fraction of closed RCs, denoted by x , is continuously increasing with time t . The bunching of closed RCs is manifested in the nonvanishing form of the near-site connected correlations, which was studied in Ref. [14]. With increasing time, i.e., with increasing value of x , the typical size of clusters of closed RCs increases, and at a critical concentration x_c , a percolation transition takes place. In this paper we ask how the parameters of the model (the hopping probability p and the lifetime of the exciton n) affect the properties of the percolation transition. We perform extensive Monte Carlo (MC) simulations and calculate the spanning probability for different boundary conditions and spanning rules, and in this way we determine the value of the percolation threshold x_c and the correlation length critical exponent ν . At the critical point the fractal properties of the giant cluster are studied, both in the bulk and at the surface.

The rest of the paper is organized in the following way. The model and its known properties are introduced in Sec. II. Results of MC simulations are presented in Sec. III and discussed in Sec. IV.

II. EXCITON MIGRATION MODEL

To define the EM model for photosynthetic bacteria we use the concept of photosynthetic units (PSUs) [5]. In a simplified picture each PSU has a reaction center and a light-harvesting

* dauriac@neel.cnrs.fr

† igloi.ferenc@wigner.hu

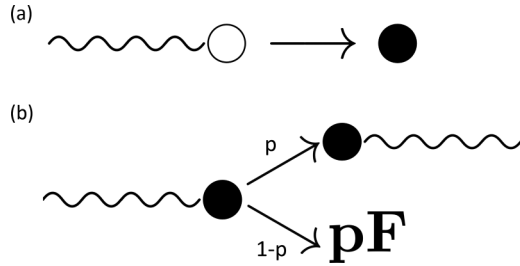


FIG. 1. Illustration of the processes between an exciton (represented by a wavy line) and an RC. (a) If the RC is open (represented by an open circle), it will become closed (represented by a solid circle). (b) If the RC is closed, the exciton is redirected with probability p , or its energy is dissipated by emission of a fluorescence quantum (represented by pF) with probability $(1 - p)$.

antenna. In the EM model the PSUs are assumed to occupy the sites of a lattice: $i = 1, 2, \dots, N$. For simplicity, the lattice is expected to be regular, with a coordination number z , and in the present case we consider the square lattice. To each RC a two-state variable $\sigma_i = \{0, 1\}$ is assigned, with $\sigma_i = 0$ for the open RC and $\sigma_i = 1$ for the closed RC. The control parameter of the process is the fraction of closed RCs, which is defined as $x = \langle \sigma \rangle = \lim_{N \rightarrow \infty} 1/N \sum_{i=1}^N \sigma_i$ and will be called occupancy in the following. The control parameter is time dependent, $x = x(t)$, and monotonously increases with t . At the starting point all RCs are open, and thus, $x(0) = 0$; after sufficiently long time all RCs became closed, $x(t) = 1$ for $t > t^*$.

A. Relaxation process

In the relaxation process we start from a fully closed state, and after a sufficient period of time, a fraction of the RCs $(1 - x)$ will spontaneously reopen. Using an appropriate weak probing light beam, the dynamics of the system can be studied in this case, too. The structure of the closed RCs is different in induction and in relaxation. In the latter process the closed sites are uncorrelated [like in ordinary (inverse) percolation], but in induction there is bunching of near-staying closed sites. This difference in the structure of the closed RC clusters leads to a hysteresis in the fluorescence spectrum, as demonstrated recently in Ref. [14]. In this paper in the following we restrict ourselves to the induction process.

B. Induction process

In induction, if an incoming exciton hits an open RC it will become closed [see Fig. 1(a)]. If, however, the exciton hits a closed RC, two processes can take place. With probability p , the exciton is redirected to a neighboring RC, or with probability $(1 - p)$ the energy of the exciton is dissipated by emission of a fluorescence quantum [see Fig. 1(b)]. If the exciton is redirected from a closed RC, the processes in Fig. 1 are repeated until the lifetime of the exciton. This means that it can visit at most n closed RCs during this wandering. Regarding the exciton wandering, we assume that the exciton can jump to only the nearest neighbors, and it can also visit the same closed RC several times.

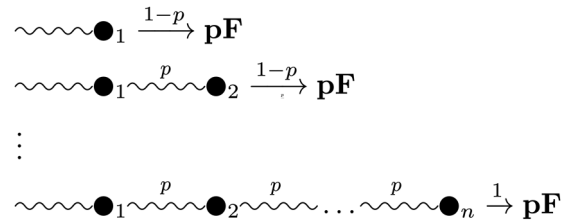


FIG. 2. Illustration of the processes yielding fluorescence. First line: one-step process with the contribution $(1 - p)G_1$. Second line: two-step process with the contribution $(1 - p)pG_2$. Third line: n -step process with the contribution $p^{n-1}G_n$ since the energy of the exciton is radiated with probability 1. G_k are multisite correlation functions of closed RCs, which are defined in the text. Note that for $k \geq 3$ step walks the same closed RC can be visited several times.

C. Fluorescence yield

The fluorescence yield φ is the sum of the contributions of $k = 1, 2, \dots, n$ step exciton walks, as illustrated in Fig. 2. This is given by

$$\varphi = \sum_{k=1}^{n-1} (1 - p)p^{k-1}G_k + p^{n-1}G_n \tag{1}$$

in terms of the multisite correlation functions G_k . They are the fraction of such k -step random walks which visit (nearest-neighbor) closed RCs and will be approximated in the following paragraphs [see Eqs. (3), (4), and (5)].

Evidently, the case $n = 1$ or $p = 0$ is special, in which the exciton is not redirected from a closed RC and the fluorescence yield is given simply as $\varphi = G_1 = \langle \sigma \rangle = x$. In this case the structure of clusters follows uncorrelated percolation. However, for $n > 1$ (and $p > 0$) the multisite correlations are nonzero, $G_k \neq 0$, $k > 1$, and there are correlations between the sites of the clusters.

The dynamics of closing the open RCs follows from the fact that all incoming photons that are not emitted through fluorescence will reduce the number of open RCs. Thus, the time dependence of x follows the rule

$$\frac{dx}{dt} = 1 - \varphi, \tag{2}$$

where the photochemical rate constant (time-scaling factor) is set $k_I = 1$.

D. Analytical methods

In an analytical treatment to integrate the equation in Eq. (2) one needs to use some approximation for the multisite correlation functions. In Joliot theory *standard mean-field approximation* is used:

$$G_k \approx x^k, \quad n \rightarrow \infty, \tag{3}$$

so that the exciton can hop to any site and its lifetime is unlimited.

The local topology of the lattice, as well as the finite lifetime of the exciton, is taken into account in the *lattice mean-field approximation*, in which case the multisite

correlation functions are written in the form

$$G_k \approx \sum_{j=2}^k c_j^{(k)} x^j. \tag{4}$$

Here $c_j^{(k)} z^{k-3}$ is the number of $(k \geq 2)$ -step random walks which have visited $2 \leq j \leq k$ different sites, where the walker arrives at the lattice in the first step. For a square lattice with $z = 4$ the first few terms of $c_j^{(k)} z^{k-3}$ are given in Ref. [14]. This approximation is expected to be correct in the relaxation process.

In induction the bunching of closed RCs is important, which is taken into account in the *cluster mean-field approximation*. In this case the multisite correlation functions are approximated in terms of two-site functions, x_2 , and the density, x , as

$$G_k \approx \sum_{j=2}^k c_j^{(k)} \frac{x_2^{j-1}}{x^{j-2}}, \tag{5}$$

and x_2 was calculated analytically in Ref. [14].

E. Monte Carlo simulations

In this paper the time evolution of x and the structure of the closed RC clusters are studied through MC simulations. The RCs are considered to sit on sites of square lattices of size $L \times L$ with $L = 2^l$, $l = 7, 8, \dots, 14$, and both free and periodic boundary conditions are used. The external light source is expected to emit one photon per time step at discrete times: $t = \tau, 2\tau, \dots, m\tau, \dots$, and immediately, one exciton starts to move from a randomly selected position of the lattice. Following the rules in Fig. 1, the exciton takes at most n steps, during which at most one open RC will be closed. We record the order parameter $x(t)$ and the structure of the closed RC clusters, for which the Hoshen-Kopelman algorithm [20] is used. Particular attention is paid to the properties of the largest cluster. For each size the results are averaged over 10^4 independent realizations. Since the algorithm involves the neighbors of a site, the boundary condition has to be chosen before starting the construction of the sample. This is in contrast to the traditional percolation process (which is the case for $n = 1$ or $p = 0$), where the boundary condition is necessary only to analyze the samples.

III. RESULTS OF THE PERCOLATION TRANSITION IN THE EM MODEL MODEL

As the fraction of closed RCs x increases, connected clusters are formed. These clusters are characterized by a typical mass (number of closed RCs) $m(x)$ and a typical linear size $\xi(x)$; both monotonously increase with x . At a critical value, $x = x_c$, a giant cluster is formed, and its size becomes divergent as $\xi(x) \sim (x_c - x)^{-\nu}$, with ν being the correlation length critical exponent [21]. At the critical point the giant cluster is a fractal, its mass is related to its linear size as $m(x_c) \sim \xi^{d_f}$, and d_f is the fractal dimension. The fractal structure of the giant cluster is illustrated in Fig. 3.

Above the percolation threshold, $x > x_c$, the giant cluster contains a finite fraction of sites, $P(x) > 0$, which behaves in

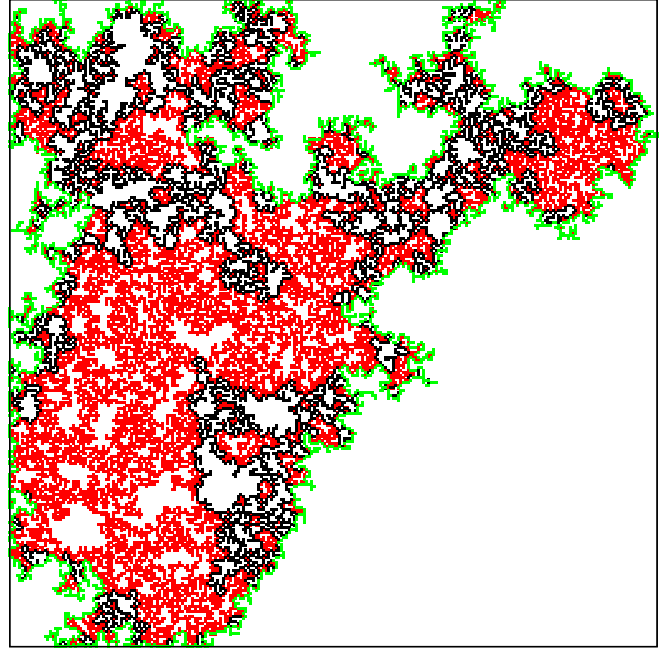


FIG. 3. Illustration of the fractal structure of the giant cluster for $n = 3$ and $p = 0.5$ at an occupancy $x = 0.589$, slightly above the percolation threshold (see Table I) for $L = 256$. Sites in the bulk are shown in red (dark gray), sites at the perimeter are indicated in green (light gray), and the hull is composed of the black and green (light gray) sites.

the vicinity of the transition point as $P(x) \sim (x - x_c)^\beta$, with a critical exponent β , the value of which follows from scaling theory [21] as $\beta = (d - d_f)\nu$. In $2d$ traditional percolation the critical exponents are [21]

$$\nu = 4/3, \quad d_f = 91/48, \quad \beta = 5/36. \tag{6}$$

We note that several other processes belong to this universality class, such as invasion percolation [22]. Here we aim to study the percolation transition of the EM model and to compare its properties with those of traditional percolation.

A. Spanning probability and critical threshold

We start to estimate the value of the percolation threshold through the calculation of the spanning probability [23–31] $R(x, L)$, which is the probability that in a given realization with an occupancy x there is a connected cluster, which spans (or percolates) a finite system of linear size L . In

TABLE I. Critical threshold values for different parameters. For traditional site percolation ($p = 0$ or $n = 1$) we have $x_c = 0.5927460$ [32,33]. In parentheses the proportion of closed sites which have been closed directly is indicated.

	$n = 2$	$n = 3$	$n = 10$
$p = 0.1$	0.5908 (0.972)	0.5908 (0.971)	0.5908 (0.971)
$p = 0.5$	0.5843 (0.881)	0.5845 (0.867)	0.5845 (0.861)
$p = 0.9$	0.5794 (0.813)	0.5796 (0.779)	0.5817 (0.746)
$p = 1$	0.5785 (0.798)	0.5800 (0.759)	0.5836 (0.712)

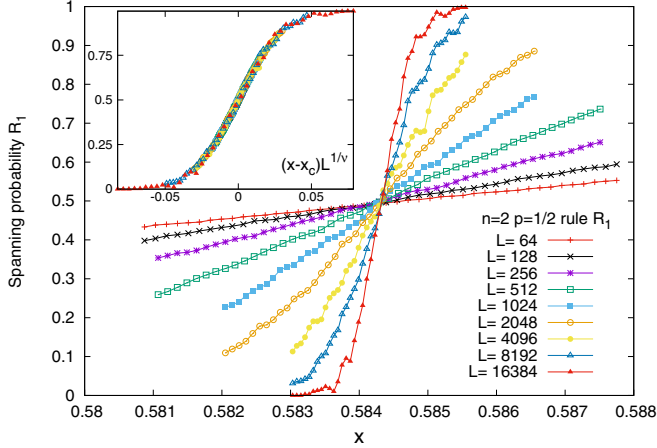


FIG. 4. Spanning probability of the EM model with $p = 0.5$ and $n = 2$ on the square lattice with open boundary conditions having the rule \mathcal{R}_1 for different linear sizes $L = 64, 128, \dots, 16\,384$, top to bottom. The crossing point of the curves defines the critical point, $x_c = 0.5843$, where $R_1(x_c, \infty) \approx 0.5$. In the inset the scaling collapse of the points averaged through duality (see text) is plotted in terms of the variable in Eq. (7).

the thermodynamic limit the spanning probability behaves as $\lim_{L \rightarrow \infty} R(x < x_c, L) = 0$ and $\lim_{L \rightarrow \infty} R(x > x_c, L) = 1$, while at the transition point it has a universal value. For finite systems in the vicinity of the transition point the appropriate scaling combination is [21]

$$\tilde{x} \sim (x - x_c)L^{1/\nu}, \quad (7)$$

and the scaling functions depend on the shape of the system, boundary conditions, and spanning rules but not on the microscopic details of the lattice.

Here we use open boundary conditions, in which case three spanning rules have been defined [24,25], which are denoted by \mathcal{R}_0 , \mathcal{R}_1 , and \mathcal{R}_2 . For \mathcal{R}_0 the cluster spans the box either horizontally or vertically; for \mathcal{R}_1 it spans the lattice in one given direction (say, horizontally), and for \mathcal{R}_2 it spans the box in both directions. For traditional percolation on the square lattice in addition there are duality relations [24,25,31]:

$$\begin{aligned} R_1(\tilde{x}) + R'_1(\tilde{x}') &= 1, \\ R_0(\tilde{x}) + R'_2(\tilde{x}') &= 1, \end{aligned} \quad (8)$$

where the primed quantities are for the dual lattice, for which $\tilde{x}' = -\tilde{x}$.

In our numerical work we have calculated the spanning probability of the EM model for different parameters $p > 0$ and $n > 1$ having rules \mathcal{R}_1 and \mathcal{R}_2 . As an illustration we show in Fig. 4 $R_1(x, L)$ for $p = 0.5$ and $n = 2$. The curves for different sizes cross each other at about the same point, which defines an estimate for the critical threshold, $x_c = 0.5843$, and a value for the critical spanning probability, $R_1(x_c, \infty) \approx 0.5$. The measured critical threshold is somewhat lower than for traditional site percolation, having $x_c = 0.5927460$ [32,33], but $R_1(x_c, \infty)$ agrees with the universal value of traditional percolation: $R_1(x_c, \infty) = 1/2$, which follows from duality and has been calculated through conformal invariance [27]. Using the estimate for x_c , the points calculated at different

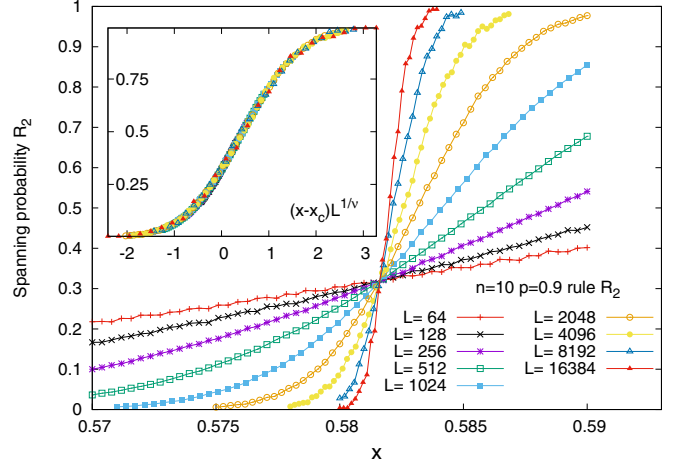


FIG. 5. Spanning probability of the EM model with $p = 0.9$ and $n = 10$ on the square lattice with open boundary conditions having the rule \mathcal{R}_2 for different linear sizes $L = 64, 128, \dots, 16\,384$, top to bottom. The crossing point of the curves defines the critical point, $x_c = 0.5817$, where $R_2(x_c, \infty) \approx 0.32$. In the inset the scaling collapse of the points is shown in terms of the variable in Eq. (7).

sizes can be put to a scaling curve in terms of the variable in Eq. (7), in which the correlation-length critical exponent for traditional percolation in Eq. (6) is used (not shown). We have also checked the possible validity of the duality relation in the first equation of Eq. (8), and in the inset of Fig. 4 we plot the quantity $\{R_1(x - x_c, L) + [1 - R_1(x_c - x, L)]\}/2$ as a function of the scaling variable \tilde{x} in Eq. (7). As seen in this inset, the duality relation is seemingly valid for the EM model, and assuming its validity, the estimate for the critical threshold could be made more accurate: $x_c = 0.58432$.

To illustrate the use of the spanning rule \mathcal{R}_2 we show in Fig. 5 the spanning probabilities for $p = 0.9$ and $n = 10$ and for different finite sizes. In this case the crossing point of the curves leads to the estimate $x_c = 0.5817$, and the measured value of the critical spanning probability, $R_2(x_c, \infty) \approx 0.32$, agrees well with the conformal result: 0.3223 [29]. Using the estimate for x_c , the points calculated at different sizes can be put to a scaling curve in terms of the variable in Eq. (7), in which the correlation-length critical exponent for traditional percolation in Eq. (6) is used (see the inset in Fig. 5).

Repeating the calculation for another set of parameters of the EM model, similar results are obtained. The critical threshold values are found to depend (weakly) on the parameters, but the critical values of the spanning probability are found to be universal for a given class of the spanning rule. The x_c values are collected in Table I, together with the fraction of points in the critical cluster which have been closed directly. At a fixed value of $n > 1$ the critical threshold monotonously decreases with increasing p , and the same is true for the fraction of directly closed points. On the other hand, at a fixed value of $0 < p \leq 1$ the n dependence of x_c is nonmonotonous; it has the minimum at $n = 2$.

B. Fractal dimensions of the critical cluster

The scaling properties of the spanning probability in the previous section indicate that the EM model probably belongs

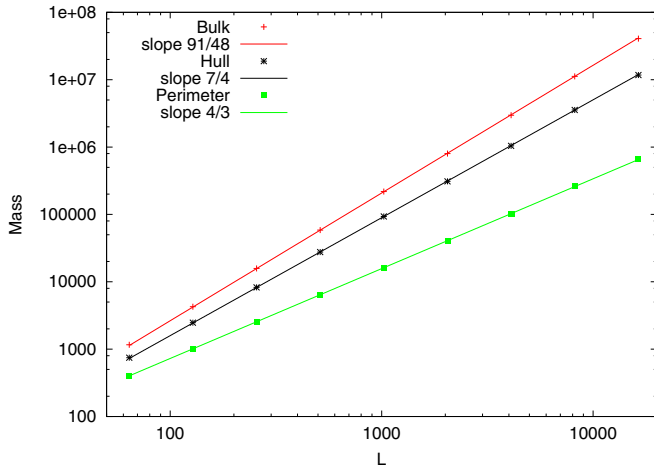


FIG. 6. Fractal properties of the critical clusters in the EM model with $p = 0.5$ and $n = 2$ on the square lattice. Average mass $m(L)$, hull $h(L)$, and perimeter $s(L)$ as a function of linear size L in log-log scale. The slope of the straight lines through the points have the fractal dimensions of traditional percolation in Eqs. (6) and (10).

to the universality class of traditional percolation. Both the values of the critical spanning probability and the correlation length critical exponent support this assumption. Here we check this point further and calculate the fractal dimension of the critical cluster, both in the bulk and at the surface.

In order to determine the bulk fractal dimension d_f , we have calculated the average mass of the critical cluster $m(L)$ for finite systems of linear size L , which is expected to scale asymptotically as $m(L) \sim L^{d_f}$. In Fig. 6 we plot $m(L)$ as a function of L in log-log scale for the EM model with $p = 0.5$ and $n = 2$. As seen in Fig. 6, the points are almost perfectly on a straight line, the slope of which is compatible with the fractal dimension of traditional percolation in Eq. (6).

Regarding the surface properties of the critical cluster, two quantities are usually studied, the hull and the perimeter [21] (see Fig. 3 for an illustration). The hull contains sites on the cluster that neighbor open sites, which are connected to the outside. On the contrary, accessible external perimeter sites of the cluster are those points which can be hit by an extended diffusing particle from outside with nonzero probability. The average number of sites on the hull and at the perimeter are denoted by $h(L)$ and $s(L)$, respectively. We have calculated both quantities for the EM model with $p = 0.5$ and $n = 2$, and they are plotted vs L in log-log scale in Fig. 6. As seen in Fig. 6 the points of both quantities are on straight lines, so we have asymptotic power-law relations:

$$h(L) \sim L^{d_h}, \quad s(L) \sim L^{d_s}. \quad (9)$$

In addition the measured slopes of the straight lines are in agreement with the known values of the fractal dimensions

for traditional percolation [34]:

$$d_h = 7/4, \quad d_s = 4/3. \quad (10)$$

IV. DISCUSSION

In this paper we examined the properties of percolation clusters formed by closed photosynthetic units of photosynthetic bacteria during light emission. The process was described in the context of an exciton migration model in which nearby sites of the clusters are closed in a correlated manner. This model contains two parameters, the exciton hopping probability p and the exciton lifetime n . After the sample has been illuminated, the fraction of closed sites $x(t)$ increases in time, and the typical (linear) size and mass of the clusters increase, too. At a critical occupancy x_c , a giant cluster is formed, and a percolation transition takes place.

In this paper the EM model was considered on the square lattice, and the properties of the percolation transition were studied through MC simulations for different values of the parameters. The critical percolation threshold was calculated by studying the spanning probability for open (and periodic) boundary conditions and for different spanning rules, \mathcal{R}_1 and \mathcal{R}_2 . The x_c values were found to vary weakly on the parameters, and the same is true for the proportion of directly closed sites (see Table I). On the other hand, the critical spanning probability was found to be universal: for a given boundary condition and a spanning rule its value is independent of the parameters of the model and corresponds to the exactly known values for (uncorrelated) traditional percolation.

From the finite-size scaling behavior of the spanning probability in the vicinity of the critical point the correlation length critical exponent ν was extracted, and its value was also found to be compatible with that of traditional percolation. We also studied the fractal properties of the critical cluster, in the bulk at the perimeter and in the hull. In each case the corresponding fractal dimensions were found to be universal; their values are compatible with the known respective values for traditional percolation.

To summarize the effect of correlations caused by the exciton migration was found to be irrelevant in the critical properties of the percolation transition of the EM model. Consequently, these correlations are sufficiently short ranged, and they do not influence the asymptotic large scale correlations in the system. This result is found to be true for both bulk and surface correlations. Similar conclusions are expected to hold for other types of lattices as well as at higher dimensions.

ACKNOWLEDGMENTS

This work was supported by the National Research Fund under Grants No. K128989 and No. KKP-126749. F.I. thanks previous cooperation in the project to P. Maróti, I. A. Kovács, M. Kis and J. L. Smart and valuable discussions with L. Gránásy.

[1] T. Mirkovic, E. E. Ostroumov, J. M. Anna, R. van Grondelle, Govindjee, and G. D. Scholes, Light absorption and energy

transfer in the antenna complexes of photosynthetic organisms, *Chem. Rev.* **117**, 249 (2016).

- [2] P. Maróti and Govindjee, Energy conversion in photosynthetic bacteria, *Photosynth. Res.* **127**, 257 (2016).
- [3] P. Maróti, Chemical rescue of H⁺ delivery in proton transfer mutants of reaction center of photosynthetic bacteria, *Biochim. Biophys. Acta, Bioenerg.* **1860**, 317 (2019).
- [4] P. Maróti, Thermodynamic view of proton activated electron transfer in the reaction center of photosynthetic bacteria, *J. Phys. Chem. B* **123**, 5463 (2019).
- [5] J. Franck and E. Teller, Migration and photochemical action of excitation energy in crystals, *J. Chem. Phys.* **6**, 861 (1938).
- [6] R. A. Niederman, Development and dynamics of the photosynthetic apparatus in purple phototrophic bacteria, *Biochim. Biophys. Acta* **1857**, 232 (2016).
- [7] W. J. Vredenberg and L. N. M. Duysens, Transfer and trapping of excitation energy from bacteriochlorophyll to a reaction center during bacterial photosynthesis, *Nature (London)* **197**, 355 (1963).
- [8] P. Joliot, P. Bennoun, and A. Joliot, New evidence supporting energy transfer between photosynthetic units, *Biochim. Biophys. Acta* **305**, 317 (1973).
- [9] G. Paillotin, Capture frequency of excitations and energy transfer between photosynthetic units in the photosystem II, *J. Theor. Biol.* **58**, 219 (1976).
- [10] D. I. G. Bennett, G. R. Fleming, and K. Amarnath, Energy-dependent quenching adjusts the excitation diffusion length to regulate photosynthetic light harvesting, *Proc. Natl. Acad. Sci. USA* **115**, E9523 (2018).
- [11] J. Lavergne and H. W. Trissl, Theory of fluorescence induction in photosystem II: Derivation of analytical expressions in a model including exciton-radical-pair equilibrium and restricted energy-transfer between photosynthetic units, *Biophys. J.* **68**, 2474 (1995).
- [12] M. de Rivoyre, N. Ginet, P. Bouyer, and J. Lavergne, Excitation transfer connectivity in different purple bacteria: A theoretical and experimental study, *Biochim. Biophys. Acta* **1797**, 1780 (2010).
- [13] H. W. Trissl, Antenna organization in purple bacteria investigated by means of fluorescence induction curves, *Photosynth. Res.* **47**, 175 (1996).
- [14] P. Maróti, I. A. Kovács, M. Kis, J. L. Smart, and F. Iglói, Correlated clusters of closed reaction centers during induction of intact cells of photosynthetic bacteria, *Sci. Rep.* **10**, 14012 (2020).
- [15] W. T. F. Den Hollander, J. G. C. Bakker, and R. van Grondelle, Trapping, loss, and annihilation of excitations in a photosynthetic system. I. Theoretical aspects, *Biochim. Biophys. Acta* **725**, 492 (1983).
- [16] F. Fassioli, A. Olaya-Castro, S. Scheuring, J. N. Sturgis, and N. F. Johnson, Energy transfer in light-adapted photosynthetic membranes: From active to saturated photosynthesis, *Biophys. J.* **97**, 2464 (2009).
- [17] K. Amarnath, D. I. G. Bennett, A. R. Schneider, G. R. Fleming, Multiscale model of light harvesting by photosystem II in plants, *Proc. Natl. Acad. Sci. USA* **113**, 1156 (2016).
- [18] J. Chmeliov, G. Trinkunas, H. van Amerongen, and L. Valkunas, Excitation migration in fluctuating light-harvesting antenna systems, *Photosynth. Res.* **127**, 49 (2016).
- [19] P. Sebban and J. C. Barbet, Simulation of the energy migration in the antenna of purple bacteria by using the Monte Carlo method, *Photobiochem. Photobiophys.* **9**, 167 (1985).
- [20] J. Hoshen and R. Kopelman, Percolation and cluster distribution. I. Cluster multiple labeling technique and critical concentration algorithm, *Phys. Rev. B* **14**, 3438 (1976).
- [21] D. Stauffer and A. Aharony, *Introduction to Percolation Theory* (Taylor and Francis, London, 1994).
- [22] D. Wilkinson and J. F. Willemsen, Invasion percolation: A new form of percolation theory, *J. Phys. A* **16**, 3365 (1983).
- [23] J. Roussenoq, J. Clerc, G. Giraud, E. Guyon, and H. Ottavi, Size dependence of the percolation threshold of square, and triangular network, *J. Phys. Lett.* **37**, 99 (1976).
- [24] P. J. Reynolds, H. E. Stanley, and W. Klein, Percolation by position-space renormalisation group with large cells, *J. Phys. A* **11**, L199 (1978).
- [25] P. J. Reynolds, H. E. Stanley, and W. Klein, Large-cell Monte Carlo renormalization group for percolation, *Phys. Rev. B* **21**, 1223 (1980).
- [26] P. D. Eschbach, D. Stauffer, and H. J. Herrmann, Correlation-length exponent in two-dimensional percolation and Potts model, *Phys. Rev. B* **23**, 422 (1981).
- [27] J. L. Cardy, Critical percolation in finite geometries, *J. Phys. A* **25**, L201 (1992).
- [28] R. M. Ziff, Spanning Probability in 2D Percolation, *Phys. Rev. Lett.* **69**, 2670 (1992).
- [29] R. P. Langlands, P. Pouliot, and Y. Saint-Aubin, Conformal invariance in two-dimensional percolation, *Bull. Amer. Math. Soc.* **30**, 1 (1994).
- [30] A. Aharony and J.-P. Hovi, Comment on Spanning Probability in 2D Percolation, *Phys. Rev. Lett.* **72**, 1941 (1994).
- [31] J.-P. Hovi and A. Aharony, Scaling and universality in the spanning probability for percolation, *Phys. Rev. E* **53**, 235 (1996).
- [32] X. Feng, Y. Deng, and H. W. J. Blöte, Percolation transitions in two dimensions, *Phys. Rev. E* **78**, 031136 (2008).
- [33] J. L. Jacobsen, High-precision percolation thresholds and Potts-model critical manifolds from graph polynomials, *J. Phys. A* **47**, 135001 (2014).
- [34] H. Saleur and B. Duplantier, Exact Determination of the Percolation Hull Exponent in Two Dimensions, *Phys. Rev. Lett.* **58**, 2325 (1987).